On in Line X-ray Phase Contrast Imaging*

Gan Huiqing[1], Zhu Huafeng[1], Chen Jianwen[1], Gao Hongyi[1], Li Ruxin[1], Xu Zhizhan[1], Zhu Peiping[2], Wang Junyue[2], Huang Wanxia[2], Yuan Qingxi[2], Xian Dingchang[2]

1 *State Key Laboratory of High Field Laser Physics, Shanghai Institute of Optics and Fine Mechanics, Chinese Academy of Sciences, Shanghai* 201800

2 *Institute of High Energy Physics, CAS, Beijing* 100080

Abstract A theoretical analysis of the in-line X-ray phase-contrast imaging with partially coherent source is presented in detail by using ambiguity function (AF). Experimental results in different conditions are presented. By comparing with absorption image, the phase contrast show high contrast and visibility of the inner structure of biological sample.

Keywords X ray; Phase contrast imaging; Ambiguity function; Synchrotron radiation

CLCN O434; O435.1 **Document Code** A

0 Introduction

X-ray phase contrast imaging gets its rapid development in 1990s with the increasing use of synchrotron sources, which is completely different form other X-ray imaging method[1~3]. Presently, various methods for X-ray phase-contrast imaging have been proposed and demonstrated. They involved either monolithic X-ray interferometers[4,5], double-crystal diffraction arrangements[6,7] or Fresnel diffraction from a monochromatic[8~10] which are, respectively, based on the measurement of φ, $\nabla\varphi$ and $\nabla^2\varphi$, where φ is the phase shift introduced by the object. Fresnel diffraction method proposed by Wilkins and co-workers[11,12] and Snigirev and co-workers[13] is popular in many researches because of the simplicity in geometry and relatively lower technical demand in operation. The usually discussed sources include plane wave[14~16], point source[17]. Partially coherent source[18~20] is also discussed by using of Van Cittert-Zernik Theorem.

In this paper, partially coherent illumination is discussed more thoroughly by using ambiguity function (AF). The partial coherent imaging theory of in line phase contrast imaging is developed by using AF, and a uniform formula for in line phase imaging is obtained and discussed. Some experimental results are agreed with the theoretical results.

*Supported by National Science Foundation of China (NO. 60278030)

Tel: 021-69918528 Email: gaohy@mail.shcnc.ac.cn

Received date: 2005-03-08

1 Theory of partial coherent X ray phase contrast imaging

By using essentially spatially partially coherent illumination, the mutual intensity is sufficient to describe the optical system. The mutual intensity is defined as $J(x_1, y_1; x_2, y_2) = \langle \zeta(x_1, y_1)\zeta^*(x_2, y_2)\rangle$ where ζ is the analytic signal associated with a transverse component of the electric-field vector. In terms of the center and difference coordinates, the mutual intensity is expressed by

$$J(x,\Delta x;y,\Delta y)=J(x+\Delta x/2,x-\Delta x/2;\ y+\Delta/2,y-\Delta y/2) \qquad (1)$$

The ambiguity function is expressed in Fourier-transform form by the following notation

$$A(u,\Delta x;v,\Delta y)=\int J(x,\Delta x;y,\Delta y)\cdot \exp\left[-2\pi i(ux+vy)\right]dxdy \qquad (2)$$

where $\Delta u,\Delta v$ is the difference spatial frequency.

Suppose that the incoherent source has a distribution of $I_s(x,y)$ and its mutual intensity is given by

$$J(x,\Delta x;y,\Delta y)=I_s(x,y)\delta(\Delta x,\Delta y) \qquad (3)$$

Using Eq. (2) leads to the AF

$$A_s(u,\Delta x;v,\Delta y=\tilde{I}_s(u,v)\delta(\Delta x,\Delta y) \qquad (4)$$

Within the paraxial approximation, the AF of the illumination on the first grating is given by

$$A_1^{(-)}(u,\Delta x;v,\Delta y)=A_s(u,\Delta x-\lambda z_1 u;v,\Delta y-\lambda z_1 u)=\frac{1}{(\lambda z_1)^2}\tilde{I}_s\left(\frac{\Delta x}{\lambda z_1},\frac{\Delta y}{\lambda z_1}\right)\delta\left(u-\frac{\Delta x}{\lambda z_1},v-\frac{\Delta y}{\lambda z_1}\right) \qquad (5)$$

where the superscripts on A indicate the function before (−) and after (+) transmission.

To examine the coherence of illumination, the corresponding mutual intensity can be determined from A_1 as a reverse Fourier transform:

The AF behind the object is expressed in terms of the convolution integral as

$$A^{(+)}(u,\Delta x;v,\Delta y)=\int A^{(-)}(u-u',\Delta x;v-v',$$

$$\Delta y) A_o(u', \Delta x; v', \Delta y) du' dv' \qquad (6)$$

Subsituting Eq. (5) into Eq. (6), then Eq. (6) reduces to

$$A_1^{(+)}(u, \Delta x; v, \Delta y) = \frac{1}{(\lambda z_1)^2} \tilde{I}_s\left(\frac{\Delta x}{\lambda z_1}, \frac{\Delta y}{\lambda z_1}\right) \cdot A_o\left(u - \frac{\Delta x}{\lambda z_1}, \Delta x; v - \frac{\Delta y}{\lambda z_1}, \Delta y\right) \qquad (7)$$

where $A_o(\Delta u, \Delta x; \Delta v, \Delta y)$ represents the AF of the object.

Suppose the object is thin one, in the same way, the transport of the AF from the object plane to the image screen is determined by the product of the transport matrices for the propagation of z_2. Thus the AF on the image screen is given by

$$A(u, \Delta x; v, \Delta y) = A_1^{(+)}(u, \Delta x - \lambda z_2 u; v, \Delta y - \lambda z_2 v) = \frac{1}{(\lambda z_1)^2} \tilde{I}_s\left(\frac{\Delta x}{\lambda z_1} - \frac{z_2}{z_1} u, \frac{\Delta x}{\lambda z_1} - \frac{z_2}{z_1} u\right) A_o\left(u - \frac{\Delta x - \lambda z_2 u}{\lambda z_1}, \Delta x - \lambda z_2 u; v - \frac{\Delta y - \lambda z_2 v}{\lambda z_1}, \Delta y - \lambda z_2 v\right) \qquad (8)$$

Specify the object by an appropriate transmission function $t(x, y)$ and obviously, $t(x, y) = 0$ when $(x, y) \notin \Omega$.

For a weak phase object $t(x, y) = 1 + j\phi(x, y)$ and the AF of the object $A_o(u, \Delta x; v, \Delta y)$ can be expressed by

$$A_o(u, \Delta x; v, \Delta y) = F\left[t\left(x + \frac{\Delta x}{2}, y + \frac{\Delta y}{2}\right) \cdot t^*\left(x - \frac{\Delta x}{2}, y - \frac{\Delta y}{2}\right)\right] = \delta(u, v) + 2\Phi(u, v) \cdot \sin\left[\pi(u\Delta x + v\Delta y)\right] \qquad (9)$$

where F represents the Fourier Transform (FT), Φ is the FT of ϕ.

Substituting (9) into (8), the FT of the intensity on the image plane then can be given by

$$\tilde{I}(x_i, y_i) = A(u, 0; v, 0) = \frac{1}{(\lambda z_1)^2} \tilde{I}_s\left(\frac{z_2}{z_1} u, \frac{z_2}{z_1} u\right) \cdot \{\delta(Mu, Mv) + 2\Phi(Mu, Mv) \sin\{\pi\lambda f[(Mu)^2 + (Mv)^2]\}\} \qquad (10)$$

Where $M = (z_1 + z_2)/z_1$ is the coefficient of image magnification and f satisfying $1/f = 1/z_1 + 1/z_2$ is the "focal distance". This result is consistent with that given by Jing cheng[18] and Hong Yu[19] et al.

Then the image intensity distribution can be expressed as

$$I(Mx, My) \propto 1 + I_s\left(\frac{z_1 + z_2)}{z_2} x, \frac{z_1 + z_2}{z_2} y\right) * * \frac{\lambda f}{2\pi} \nabla^2 \phi(x, y) \qquad (11)$$

where $* *$ represents the two dimensional convolution. From (11) it can be seen that for spatially partial coherent in line imaging, the image contrast is proportion to the laplacian of phase shift introduced by the object. Thus the detected image shows edge enhancement. This equation is valid for arbitrary degree of spatial coherence of the source. Equation (11) can be reduced to

$$I(x, y) \propto 1 - \frac{\lambda z_2}{2\pi} \nabla^2 \phi(x, y) \qquad (12)$$

for plane wave case and

$$I(Mx, My) \propto 1 + \frac{\lambda f}{2\pi} \nabla^2 \phi(x, y) \qquad (13)$$

for the point source case, which is consistent with the results given by reference 11, and 16 respectively.

2 Experimental results

The experimental setup is shown in Fig. 1. The distance between the source and the double crystal monochromator is 43 meters, thus the X-ray beam incident on the sample can be taken as parallel light beam. The X-ray beam of synchrotron radiation becomes monochromatic after the double crystal monochromator, the X-ray is refracted by the sample and detected by an X-ray CCD. Then, a phase contrast image is obtained in a proper range of distances.

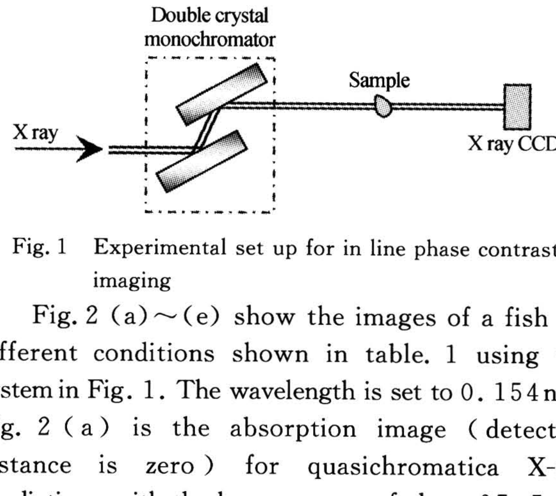

Fig. 1 Experimental set up for in line phase contrast imaging

Fig. 2 (a)~(e) show the images of a fish for different conditions shown in table. 1 using the system in Fig. 1. The wavelength is set to 0.154 nm. Fig. 2 (a) is the absorption image (detecting distance is zero) for quasichromatica X-ray irradiation, with the beam current of about 67.5 mA and exposure time of 35seconds, and (b)~(e) are the phase contrast images for different beam currents, exposure time and detecting distances. The image showed in Fig. 2(d) is detected in the same condition parameters as in Fig. 2(c) but for different side of view of the sample. To get a sufficient light exposure, in different detecting distances, the beam currency and the exposure time is adjusted correspondingly. General the lager the detecting distances, the higher the beam currencies and the longer the exposure time. Evidently the phase contrast images show an edge enhancement and show more detailed features of the inner structure of the sample, which is just coincidence with the analysis in section 2 and in other references[20]. The edge of the dark regions in the middle of these phase contrast images exhibit high brightness which indicate the edge of the fish maw, and there is a vestige of a little exposure in the region close to the edge of and no exposure in the middle of these regions , which can be interpreted that there is a large phase shift gradient in the fish maw edge, a small phase shift gradient near the fish maw edge, and no phase shift gradient around the middle of the fish maw edge of the image projection. It is because the fish is starved for days before the pictures is taken the fish maw become oblate, thus in the middle of the fish maw, there is nearly no change of accumulated refraction index, thus no exposure; while near the edge of the fish maw, there is a slow change of accumulated refractive index and according to (12), there is also a little exposure. Close to the fish bone, the images show high brightness, which indicates that there is a high value for the laplacian of the accumulated phase shift near these regions. With the increase of the detecting distance, the edge brightness is blurred which indicate that the edge enhancement is related to the detecting distance, but the influence is not obvious as theoretical simulations[16], which is because for an actual biological sample, the same region contains many different feature details, which diffract the X ray in different angles and form their only optimal images[20]. What is called the clearest image is detected in the distance corresponding to spatial frequencies characterizing the region most. It can also be clearly seen that the phase contrast images have much higher contrast than absorption images. Several regions around the fish eyes and the gill in the head show great brightness, which indicate that the phase shifts changes are the most rapid for the whole projection image and that there is a great change in either the component elements or the elements density in these regions. The broad-brush in black showed by black arrows is the noise introduced by the crystal used in experiments.

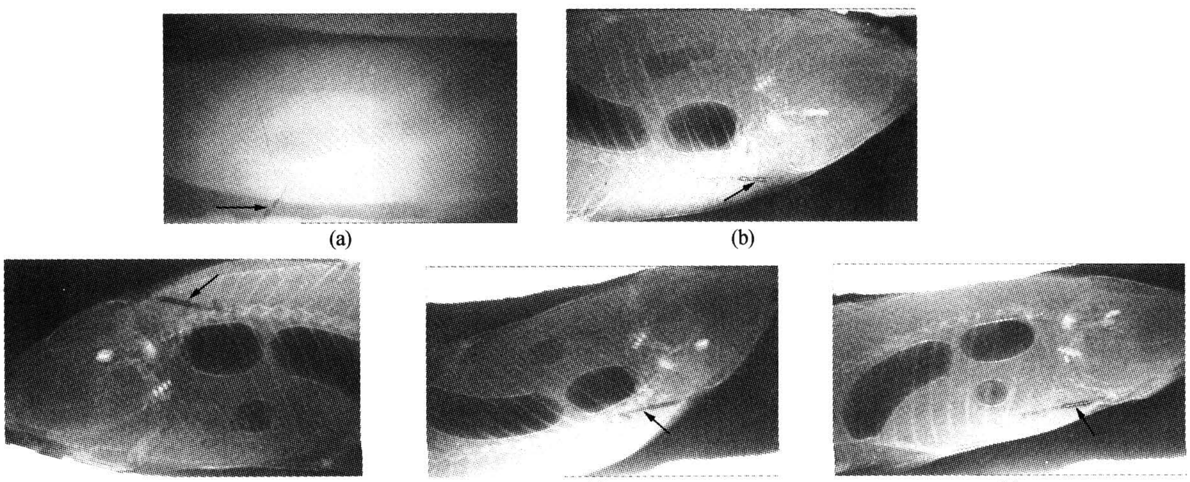

(a) (b) (c) (d) (e)

Fig. 2 In line phase contrast images using the set up shown in Fig. 1 for different conditions in shown in table. 1

Table. 1(λ=0. 154 nm)

	(a)	(b)	(c)	(d)	(e)
Beam current/mA	65. 7	62. 7	55	55	86. 5
Exposure time/s	35	5	10	10	8
Detecting distance/m	0	0. 5	0. 8	0. 8	1. 22

3 Conclusion

It has applied the ambiguity function to the analysis of spatially partial coherent in line phase contrast imaging. According to the theoretical result, the contrast of an image of a pure phase object illuminated by a spatially partial coherent wave is proportional to the Laplacian of the phase distribution on the object plane and also depends on the source-to-object and object-to-image distances. In the situation of nonuniform illumination, the influence of the intensity variation in the object plane on the image contrast is explicitly described by the derived formula.

References

1 Zhao B S, Wang J F, Gui J B. Pulse X-ray source and time-gated imaging. *Acta Photonica Sinica*, 2003, **32**(12):1450～1452

2 Zhao J, Zhu Y, Liang C, *et al*. Study of the uneven surface issue and its calibration method in the digital X-ray image. *Acta Photonica Sinica*, 2002, **31**(10):1244～1247

3 Wang Y, Du H L, Wang J J, *et al*. Analysis of image information transfer properties of X-ray intensifying screen, *Acta Photonica Sinica*, 1999, **28**(2):155～160

4 Bonse U, Hart M. AN X-ray Interferometer. *Appl Phys Lett*, 1965, **6**(8): 155～156

5 Momose A. Demonstration of phase-contrast X-ray computed tomography using an X-ray interferometer.

Nucl Instrum. *Methods Phys Res A*, 1995, **353**(3): 622～628

6 Davis T J, Gao D, Gureyev T E, *et al*. Phase-contrast imaging of weakly absorbing materials using hard X-rays. *Nature*, 1995, **373**(6515): 595～598

7 Ingal V N, Beliaecskaya E A. X-ray plane-wave topography observation of the phase contrast from a non-crystalline object. *J Phys D*, 1995, **28**(11): 2314～2318

8 Snigirev A, Snigireva I, Kohn V, *et al*. On the possibilities of x-ray phase contrast microimaging by coherent high-energy synchrotron radiation. *Rev Sci Instrum*, 1995, **66**(12): 5486～5492

9 Cloetens P, Barrett R, Baruchel J, *et al*. Phase objects in synchrotron radiation hard x-ray imaging. *J Phys D*, 1996, **29**(1): 133～147

10 Chen Min, Xiao Tiqiao, Luo Yuyu, *et al*. Phase-contrast imaging with microfocus x-ray source. *Acta Phys Sin*, 2004, **53**(9): 2953～2957

11 Wilkins S W, Gureyv T E, Gao D, *et al*. Phase-contrast imaging using polychromatic hard X-rays. *Nature*, 1996, **384**(6607): 335～338

12 Pogany A, Gao D, Wilkins S W. Contrast and resolution in imaging with a microfocus x-ray source. *Rev Sci Instrum*, 1997, **68**(7): 2774～2782

13 Raven C, Snigirev A, Spanne P, *et al*. Phase-contrast microtomography with coherent high-energy synchrotron X rays. *Appl Phy Lett*, 1996, **69**(13): 1826～1828

14 Arfelliy F, Assantez M, Bonvicinix V, *et al*. Low-dose phase contrast x-ray medical imaging. *Phys Med Biol*, 1998, **43**(10): 2845～2852

15 Gureyev T E, Pogany A, Paganin D M, *et al*. Linear algorithms for phase retrieval in the Fresnel region. *Optics Communications*, 2004, **231**(1-6): 53～70

16 Gureyev T E. Composite techniques for phase retrieval in the Fresnel region. *Optics Communications*, 2003, **220**(1-3): 49～58

17 Gureyev T E, Wilkins S W. On X-ray phase imaging with a point source. *J Opt Soc Am A*, 1998, **15**(3): 579～585

18 Cheng Jing, Han Shensheng. Phase imaging with partially coherent X rays. *Opt Lett*, 1999, **24**(3): 175～177

19 Yu Hong, Zhu Pinpin, Han Shensheng, *et al*. In-line phase-contrast imaging using partially coherent hard X-ray. *Chinese Physics Letters*, 2003, **20**(2): 220-222

20 Zhu Huafeng, Xie Honglan, Gao Hongyi, *et al*. Near-field X-ray phase contrast imaging and phase retrieval algorithm. *Chiese Physics*, 2005, **14**(4): 796～801

关于 X 射线同轴位相衬度成像的研究

干慧菁[1] 朱化凤[1] 陈建文[1] 高鸿奕[1] 李儒新[1] 徐至展[1]
朱佩平[2] 王寯越[2] 黄万霞[2] 袁清习[2] 冼鼎昌[2]
(1 中国科学院上海光学精密机械研究所，强场激光物理国家重点实验室，上海 201800)
(2 高能物理所，北京 100080)

收稿日期：2005-03-08

摘 要 利用模糊函数对部分相干源相 X 射线衬成像进行了详细的理论分析．列举了不同条件下的实验结果．通过与吸收成像相比较，相衬成像无疑对生物样品的内部结构有更高的对比度和可见度．

关键词 X 射线；相衬成像；模糊函数；同步辐射

Gan Huijing was born in 1981. She got her B. S. degree at physics department of East China Normal University in 2003. Now she is pursuing her M. S. degree in Shanghai Institute of Optics and Fine Mechanics. Her research presently focuses on X-ray imaging.